A Reaction-Diffusion Cellular Automata Model for Mycelium-based Engineered Living Materials Evolution

Ioannis Tompris[1], Ioannis K. Chatzipaschalis[1,2], Theodoros Panagiotis Chatzinikolaou[1], Iosif-Angelos Fyrigos[1], Michail-Antisthenis Tsompanas[3], Andrew Adamatzky[3], Phil Ayres[4], and Georgios Ch. Sirakoulis[1]

[1] Democritus University of Thrace, DUTH University Campus, 67100 Xanthi, Greece
[2] Universitat Politècnica de Catalunya, 08034 Barcelona, Spain
[3] University of the West of England, Bristol, UK
[4] Chair for Biohybrid Architecture, Institute of Architecture and Technology, Royal Danish Academy, 1435 København K, Denmark

Abstract. Engineered living materials (ELMs) and, more specifically, mycelium-based ELMs have been proposed as a solution to address the escalating societal pressures related to human-induced environmental disruption, scarcity of resources, and the anticipated increase in material demand. However, due to the complex biological mechanisms they emulate, their environmental sensitivity, slow supply chain and regulations, these devices present significant challenges for reproduction. Consequently, modeling the phenomena underlying such devices becomes critically important. In this context, we introduce a comprehensive mycelium-based ELM framework that incorporates reaction-diffusion processes and the modeling tool of Cellular Automata (CA). This framework successfully simulates the ELM's unpredictable growth mechanisms and closely resembles the mycelium's biological structure through the exploitation of the reaction-diffusion activator-inhibitor system. Finally, an augmented 3D version is presented that enhances the realism of our findings and strives to provide a deeper understanding of such materials.

Keywords: Cellular Automata · Reaction-Diffusion · Mycelium-based ELMs · 2D and 3D Modeling

1 Introduction

Engineered Living Materials (ELMs) represent an innovative and burgeoning area of research, distinguished by their remarkable capacity to incorporate the self-healing, regenerative, and adaptive properties inherent to biological systems with the robust and versatile structural capabilities, emblematic of materials science [21]. This interdisciplinary approach enables the development of dynamic materials that can adapt, evolve, and respond to environmental stimuli, mirroring the inherent functionalities of living organisms while maintaining the strength and reliability of engineered substances. Additionally, ELMs are utilized in designing biosensors that offer sensitive, selective, and biocompatible

solutions for health and environmental monitoring [23], [20], [26]. This demonstrates ELMs' versatility and their revolutionary potential in various applications.

Out of all the ELMs, mycelium-based ones stand out and are the primary focus of this work [10], [14], [2]. Mycelium, the vegetative part of a fungus, is renowned for its rapid growth and sustainability, presenting an eco-friendly alternative to traditional materials while also being in abundance in nature [4]. Mycelium-based ELMs are being increasingly applied across a wide range of sectors, showcasing their ability to innovate upon traditional materials science. Their uses include creating self-healing biofilms that improve durability [10], developing microgels for drug delivery and soft robotics [19], enhancing 3D printing for complex bioactive constructs [5], and producing nanofibers through electrospinning for biomedical applications and electronics [13].

However, their practical implementation is proven to be a difficult task, due to their intricate mechanisms at a microscopic level and more specifically the mycelium's tips, known as the hyphae, which exhibit behaviors such as extension, apical and lateral branching, anastomosis, nutrient uptake, and substrate diffusion, among others [11]. These mechanisms are the exact ones that we aim to replicate using reaction-diffusion (RD) systems capable of generating fractal-like patterns akin to natural mycelium networks [9], [25]. Unlike diffusion systems, which depict growth without accounting for losses and involve individually incorporating and managing each mechanism through alterations in the corresponding equations, constituting a forced growth process, reaction-diffusion systems compensate for losses via reaction processes. This results in more spontaneous growth, offering a more natural and realistic simulation of such organisms.

Towards this direction, significant research has focused on Cellular Automata (CA) over the past decades [1]. CA are computational models that utilize parallel processing capabilities and can act as distributed computational systems [3]. In CA, complex global phenomena emerge from the local interactions of simple, identical units. CA integrate computational power with mathematical and physical concepts to explore complex systems arranged as evolving cell grids with local interconnections [22]. A defining feature of CA models is their ability to demonstrate emergent behavior; this is where complex patterns and behaviors develop from simple inter-cellular rules. Moreover, the parallel computing structure inherent in CA supports a versatile and robust tool for modeling and simulating large and complex systems [29], [8], [7], providing insights into these systems' dynamics that might be unattainable through other modeling techniques and methodologies.

This work is focused on modeling the complex dynamics found in Mycelium-based ELMs, especially at the Mycelium's tip, which includes tip extension, branching, anastomosis, and nutrient uptake from the ELM's substrate. The approach involves utilizing an established RD system based on activator-inhibitor pairs [27] and modifying it to generate patterns that exhibit these dynamics. The result is a generic model that accurately represents growth in Mycelium-based ELMs. In addition, the system is constructed on a CA framework, providing a

discrete model that enhances parallelism while also providing control over the ELM's diffusion. Consequently, this results in 2D and 3D general Mycelium-based ELM models that can also be fitted to experimental data to represent the growth of biological organisms by adjusting the corresponding RD and CA parameters.

2 Mycelium-based ELM Reaction-Diffusion Mechanisms

Reaction-diffusion systems are widely used as mathematical models that describe the spatio-temporal changes and interactions between multiple substances, and as such, they are instrumental in producing complex patterns [18] and play a crucial role in understanding the formation of biological patterns [12,15]. Moreover, these models are scalable to any desired dimension because they are based on partial differential equations, which are inherently multidimensional. This characteristic is notably advantageous, as it enables the design of both two-dimensional and three-dimensional models based on these principles.

Moreover, in order to improve the understanding behind pattern formation, it is crucial to examine the details of the reaction-diffusion system employed [27]. This system outlines the dynamics between two abstract key substances depicted in Fig. 1(a), that affect the model's state: the activator and the inhibitor, and their corresponding influence on Mycelium formation. The activator encourages the Mycelium's growth on the condition that its concentration exceeds a certain threshold. On the other hand, the inhibitor acts to reduce the concentration of the activator, thus having a suppressive effect. Moreover, in Fig. 1(b) a more sophisticated point of view on the inhibitor's effect on the system is depicted, in which the inhibitor shapes the growth of the Mycelium, by managing the uncontrolled growth of the activator.

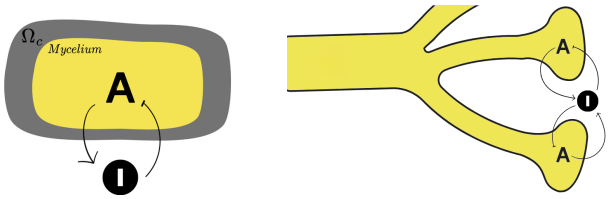

Fig. 1. (a) Activator-inhibitor dynamics. (b) The inhibitor's effect on the Mycelium's growth.

In reaction-diffusion models, activator and inhibitor pairs make it possible to simulate complex mycelial growth behaviors such as tip expansion, branching, and anastomosis. Within this framework, inhibitors manage and limit growth, whereas activators promote expansion. The outward diffusion of the activator drives the extension of mycelial hyphae by effectively replicating tip extension.

Branching emerges naturally, caused by the inhibitor's increased concentration, which gives shape to the model by preventing the contact of the activator fronts. On the other hand, when the activator's concentration is high enough, the activator fronts merge, which is similar to anastomosis, which is when hyphal tips join together.

The mathematical expressions of the RD system are given in Eqs. (1)-(4):

$$\frac{\partial u}{\partial t} = \nabla^2 u + \zeta(\kappa u + u^2 - \lambda uv), \quad where\, u \in \Omega_c \tag{1}$$

$$\frac{\partial v}{\partial t} = d\nabla^2 v + \zeta(\mu u^3 - v), \quad here\, v \in \Omega \tag{2}$$

$$\frac{dc}{dt} = \zeta\nu c(a(u) - c)(c - 1), \quad where\, c \in \Omega \tag{3}$$

$$a(u) = \begin{cases} \xi, & \text{if } u \geqslant threshold \\ \xi - \theta(u - threshold), & \text{otherwise} \end{cases} \tag{4}$$

where u and v represent the concentrations of the activator and the inhibitor, respectively. In Eq. (1) and Eq. (2), the first term on the right includes the Laplacian operator that describes how the solutions propagate through space. This term is called the diffusion term. Subsequently, the second term, which is a polynomial of u and v, elucidates the interaction between the solutions u and v, known as the reaction term. Eq. (3) describes the derivative of the mycelium state c over time, with negative values of c to highlight the presence of a mycelial tip, while $|c|$ describes the concentration of the mycelium. Tips are formed due to the extremely high and condensed concentration of the activator in a specific area, which significantly increases c. According to Eq. (3), this will result in the derivative of c to be highly negative, as ξ, which will ultimately be the value of $a(u)$, is a constant selected to be smaller than 1, thus explaining the negative value of the tips. Finally, Eq. (4) provides the function $a(u)$, which describes the dependence of the mycelium on the activator.

It is important to remember that v and c can take on values anywhere in the grid-plane $\Pi_{i,j}$, which is shown as Ω. But u can only take values in the space bounded by Ω_C, which shows a region close to c, as illustrated in Fig. 1(a). Finally, ζ, κ, λ, μ and ν are all reaction parameters that affect the corresponding interactions and ultimately influence the pattern generated. The parameters ξ and θ directly influence $a(u)$ and enable the achievement of both positive and negative gradients in the calculation of c.

3 Reaction-Diffusion CA towards 2D and 3D Simulation of Mycelium-based ELM

3.1 CA Grid Configuration

In order to use the reaction-diffusion model mentioned earlier in a discrete time and space framework that allows for a lot of parallelism and a simple, modular simulation approach, a CA framework is employed. The proposed CA-based

model uses a discrete square grid where each CA cell contains the values of u, v and c that are continuous. The activator is able to diffuse only within the space denoted by Ω_c. Ideally, u would diffuse radially adjacent to the Mycelium, to support a more natural and realistic diffusion. However, given the computational and geometric limitations of creating a circle within a discrete grid, the activator was conditionally updated, taking into account neighbors in a circular-like fashion, as depicted in Fig. 2, where in dark blue is the center cell and in light blue its corresponding neighbors.

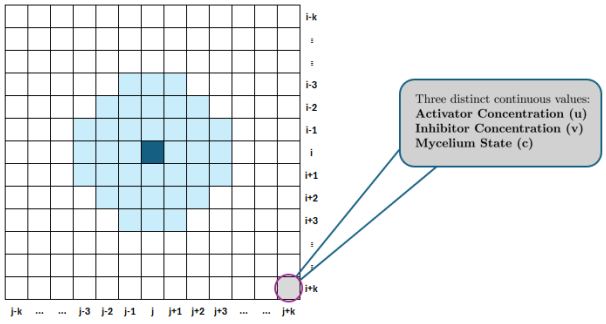

Fig. 2. Variable spaces Ω (whole grid-plane $\Pi_{i,j}$) and Ω_c (dark and light blue colors describing the referenced cell and its neighborhood accordingly) with a depth of 3 cells in the CA grid employed. In gray, a CA cell is shown containing the three continuous values that correspond to the state equations of the activator, inhibitor and mycelium.

3.2 2D and 3D Representation of the Discrete Reaction-Diffusion Process

Before we can use the diffusion processes (Eqs. 1 and 2), which are usually described by partial differential equations, in a discrete CA framework, we need to use the discrete Laplacian operator. The application of this operator is equivalent to a convolution operation with a 3×3 kernel [16].

Furthermore, by modifying the kernel's weights, the spatial growth of the activator and the inhibitor can be controlled. More specifically, it was observed that by applying two different kernels, we can achieve two different diffusion patterns in our model. The first one, which is ∇^2_A, shown in Eq. 5, results in a denser diffusion because of the increased central cell weight and ultimately in a more condensed mycelium. The second one, ∇^2_B, because of the increased neighbor interactions, describes a finer and more precise diffusion, resulting in the mycelium's tips. Alternating at the appropriate moments can create a more realistic growth pattern, depicting a condensed biomass at the center with emerging tips at the edges, similar to the morphology of biological fungi [17].

$$\nabla_A^2 = \frac{1}{20}\begin{pmatrix} 0 & 1 & 0 \\ 1 & -4 & 1 \\ 0 & 1 & 0 \end{pmatrix} \quad \nabla_B^2 = \frac{1}{100}\begin{pmatrix} 10 & 35 & 10 \\ 35 & -11 & 35 \\ 10 & 35 & 10 \end{pmatrix} \tag{5}$$

Furthermore, we can further expand the dimensionality of the model from two dimensions, which is projected on one plane $\Pi_{i,j}$, to three dimensions, projected on three perpendicular planes: $\Pi_{i,k}$, $\Pi_{i,j}$, and $\Pi_{j,k}$. Similarly with the two dimensions, a convolution operation is performed on the planes $\Pi_{i,k}$, $\Pi_{i,j}$, and $\Pi_{j,k}$ with the three kernels $\nabla_{i,k}^2$, $\nabla_{i,j}^2$, and $\nabla_{j,k}^2$, respectively. These kernels, shown in Eq. 6, are introduced in [24] and are the equivalent of the 3D discrete Laplacian operator. It is noteworthy that all other parameters remain unchanged for the 3D model. Finally, it was observed that the kernel alternation didn't affect the model's growth in three dimensions, as the number of neighbors increases exponentially, rendering a small change in some of the neighbors' weights negligible.

$$\nabla_{i,k}^2 = \frac{1}{26}\begin{pmatrix} 2 & 3 & 2 \\ 3 & 6 & 3 \\ 2 & 3 & 2 \end{pmatrix} \quad \nabla_{i,j}^2 = \frac{1}{26}\begin{pmatrix} 3 & 6 & 3 \\ 6 & -88 & 6 \\ 3 & 6 & 3 \end{pmatrix} \quad \nabla_{j,k}^2 = \frac{1}{26}\begin{pmatrix} 2 & 3 & 2 \\ 3 & 6 & 3 \\ 2 & 3 & 2 \end{pmatrix} \tag{6}$$

3.3 Algorithm for Implementing the Mycelium-based ELM Model

The algorithm detailing the model is depicted as Algorithm 1. Initially, the setting of hyperparameters (including total iterations and grid size) and the reaction-diffusion parameters takes place. Following, the concentrations of the activator, the inhibitor, and the Mycelium are initialized. The initialization of those three components is restricted to a small region in the center of the grid in order to observe and grasp the Mycelium's growth in all possible directions. Furthermore, all three components must have an initial value: the Mycelium requires the activator to grow, the activator can only propagate within the region defined by the Mycelium, and the inhibitor must be introduced into the system for the RD processes to function. It should be noted that the initialization within the central area is conducted randomly, and given the sensitivity of reaction-diffusion systems [28], the initial randomness is propagated throughout the developing pattern with each iteration.

Moreover, the simulation incorporates a substrate that varies in its capacity to support mycelium's growth, being either more or less conducive. This is integrated as a matrix which ranges from 0 to 1, that is multiplied to the reaction part u (line 19) and either promotes or suppresses it, affecting in turn c. As a result, more fertile areas are instantiated with a higher value, while less fertile areas get a rather small non-zero value. The model also randomly introduces obstacles, such as rocks within the substrate, which are clusters of zeros inside the matrix that impede the activator's (u) development and, consequently, the growth of the Mycelium in those specific areas.

The CA model then initiates a loop phase where its state is continuously updated. Initially, Ω_c is established based on the neighborhood defined in Fig. 2. Then, Ω_c is iteratively updated at each simulation step to represent the confined area in which the activator can take values, resulting in the activator gradually expanding in a circular pattern. The "for loops" in lines 9 and 10 do not iterate over the whole grid to prevent overflow, due to the considerable size of Ω_c. Next, in line 18, a kernel between ∇^2_A and ∇^2_B is chosen to control the diffusion of u and v. This is equivalent to a change in the CA's rule update. Subsequent processes include the conditional and unconditional update of the activator and the inhibitor, respectively (lines 17-20). Following, function $\alpha(u)$ is computed to determine the concentration of the mycelium c at each time step (lines 21-25). Lastly, concentration limiters are used to make sure that both the activator and the suppressor diffuse properly, as discussed in Section 3.1.

Algorithm 1 Mycelium-based ELM Model

1: $grid \leftarrow 800$
2: $iterations \leftarrow totalIterations$
3: $\{\theta, \zeta, \kappa, \lambda, \mu, \nu, \xi, \mathrm{amax}, \mathrm{imax}, threshold\} \leftarrow \{2.5, 625, 0.5, 0.8, 2.6, 1, 0.49, 20, 30, 0.5\}$
4: $u,\ v,\ c \leftarrow and(size(10))$
5: $substrate \leftarrow rand(size(grid))$
6: $step,\ i,\ j\,(counters) \leftarrow 0$
7: $\Omega_c \leftarrow 0$
8: **for** `step < iterations` **do**
9: **for** `i < (grid-length(`Ω_c`))` **do**
10: **for** `j < (grid-length(`Ω_c`))` **do**
11: **if** $c(i,j) > 0$ **then**
12: $\Omega_c(i,j) \leftarrow 1$
13: **end if**
14: **end for**
15: **end for**
16: **for** `i < grid` **do**
17: **for** `j < grid` **do**
18: `rule alternate`
19: **if** $\Omega_c(i,j) == 1$ **then**
20: $u_{new}(i,j) \leftarrow u_{old}(i,j) + \nabla^2 u_{old}(i,j) + substrate \cdot \zeta(\kappa u_{old}(i,j) + u_{old}(i,j)^2 - \lambda u_{old}(i,j) v_{old}(i,j))$
21: **end if**
22: $v_{new}(i,j) \leftarrow v_{old}(i,j) + +d\nabla^2 v_{old}(i,j) + \zeta(\mu u_{old}(i,j)^3 - v_{old}(i,j))$
23: **if** $u_{new}(i,j) \geqslant threshold$ **then**
24: $a(u_{new}(i,j)) \leftarrow \xi$
25: **else**
26: $a(u_{new}(i,j)) \leftarrow \xi - \theta(u_{old}(i,j) - threshold)$
27: **end if**
28: $c_{new}(i,j) \leftarrow c_{old}(i,j) + \Omega_c \zeta \nu c_{old}(i,j)(a(u_{new}(i,j)) - c_{old}(i,j))(c_{old}(i,j) - 1)$
29: **end for**
30: **end for**
31: **if** $u_{new}(i,j) > \mathrm{amax}$ **then**
32: $\mathrm{amax} \leftarrow u_{new}(i,j)$
33: **end if**
34: **if** $v_{new}(i,j) > \mathrm{imax}$ **then**
35: $\mathrm{imax} \leftarrow v_{new}(i,j)$
36: **end if**
37: **end for**

In conclusion, the model's growth is succinctly described by a three-way interaction, in which the space Ω_c permits values for the activator, which subse-

quently stimulates the growth of the Mycelium. Following this, Ω_c is updated and expands in regions where c is non-zero. This process is repeated and establishes the use of the variable range Ω_c.

4 Simulation Results

The results of the 2D model's simulations are presented in this Section. It is clear that the 2D model can accurately replicate fundamental1 mycelium behaviors like tip extension, branching, and anastomosis, confirming its ability to mimic fungal-based ELMs. By simulating these processes, the model looks like a fungus, especially by reflecting the patterns found in fungi, especially those in the Rhizoctonia Solani family [6]. This lends credibility to the modeling results. It is noteworthy that the employed model is not used to represent specific chemical species. Instead, it serves as a mathematical framework designed to broadly and effectively capture the dynamics of the system, aiming to accurately simulate the evolution of mycelium. The involved abstract variables are employed to model the emergent patterns and behaviors seen in the ELM bio-inspired system, rather than directly representing particular chemical entities. In addition, simulation results for the 3D model, an extension of the 2D model, are presented.

4.1 2D Model Results

In Fig. 3, the CA-based mycelium's growth is depicted, which is shown at different simulation steps. One can observe the condensed biomass at the center, while the hyphae are visible at the periphery. This is accomplished by alternating between the two kernels, ∇_A^2 and ∇_B^2, in a 3:1 ratio, respectively, every 100 iterations, following in a sense the natural process. This means that, every 100 iterations, diffusion is performed with ∇_A^2 for 75 iterations and with ∇_B^2 for the remaining 25 iterations.

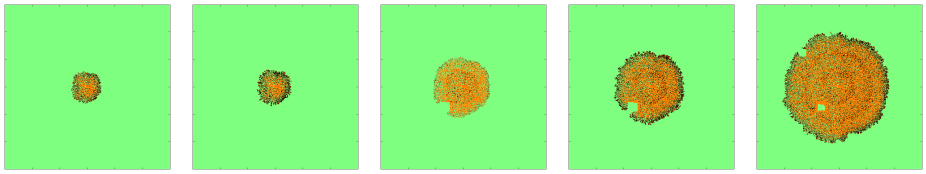

(a) 100 (b) 160 (c) 260 (d) 320 (e) 480

Fig. 3. Mycelium concentration c at different simulation steps.

Focusing on Fig. 4, the patterns of the activator, inhibitor, and mycelium are very similar. This is reasonable given that the activator's growth, which the inhibitor shapes, directly affects the mycelium's state. Furthermore, their concentration ranges are represented on the corresponding color bars. Furthermore, in areas where the substrate is more prosperous (closer to 1), there is a

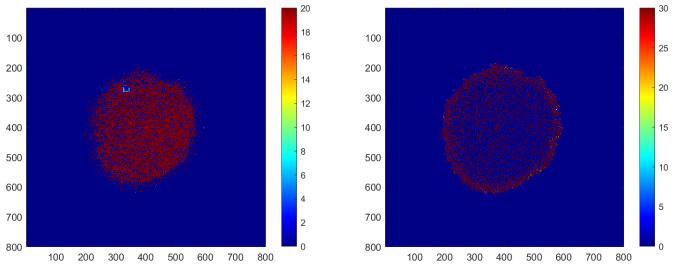

(a) Activator Concentration (b) Inhibitor Concentration

(c) Mycelium State (d) Substrate

Fig. 4. (a-c) Final patterns of the activator, inhibitor concentrations and the mycelium state respectively after 500 timesteps, and (d) substrate initialization for the 2D model.

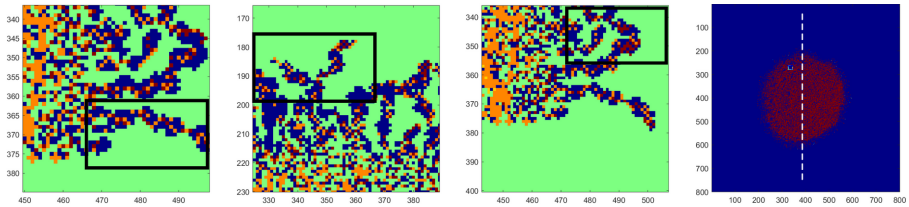

(a) Extension (b) Branching (c) Anastomosis (d) Nutrient uptake

Fig. 5. (a-c) Simulated biological mechanisms of the mycelium's hyphae depicted in the mycelium's concentration c. (d) Nutrient uptake and mycelium's density depicted in the activator's concentration u.

higher concentration of the activator, which results in a thicker cell structure. The model also randomly introduces obstacles, for example rocks, within the substrate, which impede the growth of the ELM in those specific areas.

Moreover, the fundamental mycelium-based ELM mechanisms which include hyphae extension, apical and lateral branching, anastomosis and nutrient uptake are observed and showcased in Fig. 5, which is a magnification of the Mycelium's State in Fig. 4(c). Extension, branching, and anastomosis are readily observable in the mycelium's hyphae, while nutrient uptake is indicated by the density of the

activator. The substrate morphology results in a denser right region, as shown in Fig. 4(d).

4.2 3D Model Results

In Fig. 6, the results of the 3D model simulation are presented. The augmentations consistently maintain the integrity of the 2D model's design, effectively showcasing the condensed biomass along with the precise spherical morphology of the fungi. These enhancements support the spatial and structural fidelity of the model and also underline the robustness of the model in replicating complex biological forms. The detailed visualization aids in understanding the dynamic interactions and growth patterns within the modeled environment.

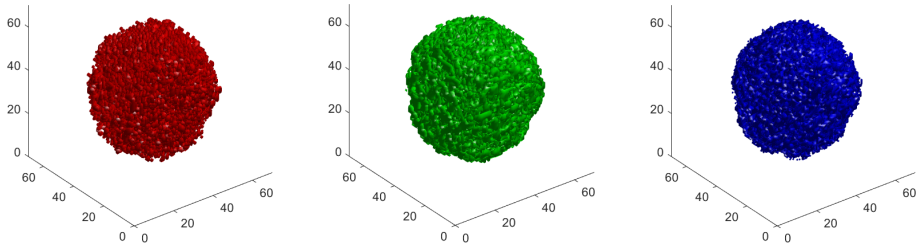

(a) Activator Concentration (b) Inhibitor Concentration (c) Mycelium State

Fig. 6. Final patterns of the activator, inhibitor concentration and the mycelium state, respectively, after 100 time steps for the 3D model.

5 Conclusions and Future Work

This paper introduces a mycelium-based ELM model, utilizing CA within their framework. The model is grounded in RD processes, which are prevalent in natural systems, providing enhanced insights into the dynamics of such organisms. It employs an activator-inhibitor interaction, capable of generating a diverse array of patterns while also extending to three dimensions. Overall, the model effectively replicates the fundamental mechanisms of mycelium, including tip extension, branching, anastomosis, and nutrient uptake, and it also exhibits characteristic bio-inspired patterns. The model alternates between different Laplacian operators in its diffusion processes in order to capture the Mycelium's essence, which includes a condensed central biomass and discernible tips at its edges. Both 2D and 3D simulation results reflect the pattern observed in the biological fungi, validating the results of the proposed reaction-diffusion CA model.

Future work will involve inclusion of external factors such as temperature and electrical stimuli, among others, using the reaction-diffusion's capabilities

for dynamic interactions. Such a system could be enhanced by moving it to a Field Gate Programmable Array (FPGA) board, which can provide significant simulation parallelism and a real-time interaction with those external factors by utilizing the board's Analog to Digital Converters (ADCs). Additionally, a mycelium-based ELM with bacterial symbiosis will be developed to improve control and structural properties, advancing the study of biologically inspired systems.

Acknowledgments This work has been supported by the framework of the FUNGATERIA project, which has received funding from the European Union's HORIZON-EIC-2021-PATHFINDER CHALLENGES program under grant agreement No. 101071145.

References

1. Adamatzky, A.: Cellular automata: a volume in the encyclopedia of complexity and systems science. Springer Publishing Company, Incorporated (2018)
2. Adamatzky, A.: Fungal machines: Sensing and computing with fungi, vol. 47. Springer Nature (2023)
3. Ahangaran, M., Taghizadeh, N., Beigy, H.: Associative cellular learning automata and its applications. Applied Soft Computing **53**, 1–18 (2017)
4. Angelova, G.V., Brazkova, M.S., Krastanov, A.I.: Renewable mycelium based composite – sustainable approach for lignocellulose waste recovery and alternative to synthetic materials – a review. Zeitschrift für Naturforschung C **76**(11-12), 431–442 (2021)
5. Antinori, M.E., Contardi, M., Suarato, G., Armirotti, A., Bertorelli, R., Mancini, G., Debellis, D., Athanassiou, A.: Advanced mycelium materials as potential self-growing biomedical scaffolds. Scientific Reports **11**(1), 12630 (Jun 2021)
6. Boswell, G.P.: Modelling mycelial networks in structured environments. Mycological Research **112**(9), 1015–1025 (2008)
7. Chatzinikolaou, T.P., Fyrigos, I.A., Ntinas, V., Kitsios, S., Bousoulas, P., Tsompanas, M.A., Tsoukalas, D., Adamatzky, A., Sirakoulis, G.C.: Wave cellular automata for computing applications. In: 2022 IEEE International Symposium on Circuits and Systems (ISCAS). pp. 3463–3467. IEEE (2022)
8. Chatzipaschalis, I.K., Chatzinikolaou, T.P., Fyrigos, I.A., Adamatzky, A., Rubio, A., Sirakoulis, G.C.: Memristor-based cellular automata for natural language processing. In: 2023 30th IEEE International Conference on Electronics, Circuits and Systems (ICECS). pp. 1–4. IEEE (2023)
9. Davidson, F., Sleeman, B., Rayner, A., Crawford, J., Ritz, K.: Large-scale behavior of fungal mycelia. Mathematical and Computer Modelling **24**(10), 81–87 (1996)
10. Elsacker, E., Zhang, M., Dade-Robertson, M.: Fungal engineered living materials: The viability of pure mycelium materials with self-healing functionalities. Advanced Functional Materials **33**(29), 2301875 (2023)
11. Fricker, M.D., Heaton, L.L., Jones, N.S., Boddy, L.: The mycelium as a network. The fungal kingdom pp. 335–367 (2017)
12. Gierer, A., Meinhardt, H.: A theory of biological pattern formation. Kybernetik **12**, 30–39 (1972)

13. Heide, A., Wiebe, P., Sabantina, L., Ehrmann, A.: Suitability of mycelium-reinforced nanofiber mats for filtration of different dyes. Polymers **15**(19) (2023)
14. Karana, E., Blauwhoff, D., Hultink, E.J., Camere, S.: When the material grows: A case study on designing (with) mycelium-based materials. International Journal of Design **12**(2) (2018)
15. Kondo, S., Miura, T.: Reaction-diffusion model as a framework for understanding biological pattern formation. Science **329**(5999), 1616–1620 (2010)
16. Kong, H., Akakin, H.C., Sarma, S.E.: A generalized Laplacian of Gaussian filter for blob detection and its applications. IEEE Transactions on Cybernetics **43**(6), 1719–1733 (2013)
17. Krull, R., Cordes, C., Horn, H., Kampen, I., Kwade, A., Neu, T.R., Nörtemann, B.: Morphology of filamentous fungi: linking cellular biology to process engineering using aspergillus niger. Biosystems Engineering II: Linking Cellular Networks and Bioprocesses pp. 1–21 (2010)
18. Landge, A.N., Jordan, B.M., Diego, X., Müller, P.: Pattern formation mechanisms of self-organizing reaction-diffusion systems. Developmental Biology **460**(1), 2–11 (2020)
19. Liu, A.P., Appel, E.A., Ashby, P.D., Baker, B.M., Franco, E., Gu, L., Haynes, K., Joshi, N.S., Kloxin, A.M., Kouwer, P.H.J., Mittal, J., Morsut, L., Noireaux, V., Parekh, S., Schulman, R., Tang, S.K.Y., Valentine, M.T., Vega, S.L., Weber, W., Stephanopoulos, N., Chaudhuri, O.: The living interface between synthetic biology and biomaterial design. Nature Materials **21**(4), 390–397 (Apr 2022)
20. Liu, S., Xu, W.: Engineered living materials-based sensing and actuation. Frontiers in Sensors **1** (2020)
21. Mora-Boza, A., Acosta, S., Puertas-Bartolomé, M.: Chapter 9 - biopolymers for the development of living materials for biomedical applications. In: Sessini, V., Ghosh, S., Mosquera, M.E. (eds.) Biopolymers, pp. 263–294. Elsevier (2023)
22. Neumann, J.V.: Theory of Self-Reproducing Automata. University of Illinois Press (1966)
23. Nguyen, P.Q., Courchesne, N.M.D., Duraj-Thatte, A., Praveschotinunt, P., Joshi, N.S.: Engineered living materials: prospects and challenges for using biological systems to direct the assembly of smart materials. Advanced Materials **30**(19), 1704847 (2018)
24. O'Reilly, R.C., Beck, J.M.: A family of large-stencil discrete laplacian approximations in three-dimensions. Int. J. Numer. Methods Eng pp. 1–16 (2006)
25. Regalado, C., Crawford, J., Ritz, K., Sleeman, B.: The origins of spatial heterogeneity in vegetative mycelia: a reaction-diffusion model. Mycological Research **100**(12), 1473–1480 (1996)
26. Rodrigo-Navarro, A., Sankaran, S., Dalby, M.J., del Campo, A., Salmeron-Sanchez, M.: Engineered living biomaterials. Nature Reviews Materials **6**(12), 1175–1190 (2021)
27. Sugimura, K., Shimono, K., Uemura, T., Mochizuki, A.: Self-organizing mechanism for development of space-filling neuronal dendrites. PLOS Computational Biology **3**(11), 1–12 (11 2007)
28. Van Gorder, R.A.: A theory of pattern formation for reaction–diffusion systems on temporal networks. Proceedings of the Royal Society A: Mathematical, Physical and Engineering Sciences **477**(2247), 20200753 (2021)
29. Wolfram, S.: Cellular automata and complexity: collected papers. CRC Press (2018)